

# Development of the Bio-Optical Algorithms to Retrieve the Ocean Environmental Parameters from GOCI

Joo-Hyung, Ryu<sup>\*</sup>, Jeong-Eon Moon, Shanmugam P., Jee-Eun Min, Yu-Hwan Ahn  
Ocean Satellite Research Group  
Korea Ocean Research & Development Institute,  
Ansan P.O. Box 29, Seoul, 425-600, Korea  
jhryu@kordi.re.kr

**Abstract:** The Geostationary Ocean Color Imager (GOCI) will be loaded in Communication, Ocean and Meteorological Satellite (COMS). To efficiently apply the GOCI data in the variety of fields, it is essential to develop the standard algorithm for estimating the concentration of ocean environmental components (<chl>, <SS>, and <CDOM>). For developing the empirical algorithm, about 300 water samples and *in situ* measurements were collected from sea water around the Korean peninsula from 1998 to 2006. Two kinds of chlorophyll algorithms are developed by using statistical regression and fluorescence technique considering the bio-optical properties in Case-II waters. The single band algorithm for <SS> is derived by relationship between Rrs(555) and *in situ* concentration. The CDOM is estimated by absorption coefficient and ratio of Rrs(412)/Rrs(555). These standard algorithms will be programmed as a module of GOCI Data Processing System (GDPS) until 2008.

**Keywords:** COMS GOCI, Surface suspended sediment, Chlorophyll, Colored dissolved organic matter, GDPS

## 1. Introduction

GOCI, the first Geostationary Ocean Color Imager, shall be operated in a staring-frame capture mode onboard its Communication Ocean and Meteorological Satellite (COMS) and tentatively scheduled for launch in 2008. It is the world's first geostationary ocean color sensor. The mission concept includes eight visible-to-near-infrared bands, 0.5 km pixel resolution, and a coverage region of  $2,500 \times 2,500$  km centered at Korea. The instrument is expected to provide SeaWiFS quality observations for a single study area with imager frequency of 1 hour from 10 am to 5 pm. It is possible to monitor the abrupt change in coastal and oceanic waters covering the East Sea/Japan Sea (ES), the Yellow Sea (YS) and the East China Sea (ECS) in addition to existing function of polar-orbit ocean color satellites. The GOCI data can be used to monitor the harmful algae bloom (HAB), health of marine ecosystem, movement of suspended sediment and current, and to produce marine fisheries information to the fishing communities.

A bipartite classification scheme, according to which oceanic waters are partitioned into Case-1 or Case-2 waters, was introduced by Morel and Prieur (1977), and refined later by Gordon and Morel (1983). By definition, Case-1 waters are those waters in which phytoplankton are the principal agents responsible for variations in optical properties of the water. On the other hand, Case-2 waters are influenced not just by phytoplankton and re-

lated particles, but also by other substances, that vary independently of phytoplankton, notably inorganic particles in suspension and yellow substances. In the GOCI swath, the western coastal sea of Korea peninsula and the East China Sea (ECS) is a typical Case-2 and the East Sea and the Pacific come under the Case-1 waters. Therefore, it is essential to develop the new bio-optical algorithm suitable for complex optical properties considering Case-1 and Case-2 waters. In this study, we focused on empirical algorithms based on relationship between *in situ* ocean environmental parameters and optical measurements.

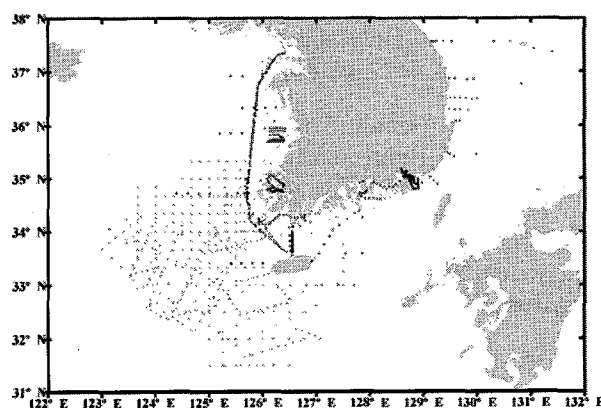


Fig. 1 Location map and sampling positions of *in situ* measurements during 8 years around the Korean Sea

## 2. Study Area and Data

The western part of GOCI swath shows the characteristics of complex Case-2 water environments of the Korean South Sea (KSS), YS, ECS and Bohai Sea (BS) determined by major physical currents such as the Kuroshio Warm Current and its branches, the Tsushima Warm Current (TWC) and Jeju Warm Current (JWC), and sub-branches the East Korean Warm Current (EKWC) along the Korean east coast and Offshore Branch (OB) along the Japanese coast (Chang et al., 2002; Lie et al., 1998). The concentrations of Chl in the surface waters of KSS normally range from 0.2 to  $72 \text{ mg m}^{-3}$  (occasionally reaching over  $100 \text{ mg m}^{-3}$ ), suspended sediments (SSC) from 0.5 to  $125 \text{ g m}^{-3}$  and dissolved organic matter (DOM) from 0.2 to  $2 \text{ m}^{-1}$ . In the ECS the 6300 km long Yangtze river drains a catchment area of

$1.96 \times 10^6 \text{ km}^2$  in China with annual discharge of  $9.8 \times 10^{11} \text{ m}^3$ , exporting abundant quantities of nutrients (annual fluxes of total inorganic nitrogen, phosphate, silicate and nitrate are  $8.88 \times 10^6 \text{ t}$ ,  $1.36 \times 10^4 \text{ t}$ ,  $2.04 \times 10^6 \text{ t}$  and  $6.36 \times 10^6 \text{ t}$  respectively) and sediments (annual sediment load is  $4.86 \times 10^8 \text{ t}$  with an average SSC level of about  $500 \text{ mg l}^{-1}$ ) to the estuary and areas in its vicinity (Shen et al., 1992; Goa and Song, 2005). The sedimentation and resuspension processes at the same time are intense due to strong tidal amplitude (an average of 4.5-5.0 m) and current ( $2.0\text{-}2.5 \text{ m s}^{-1}$ ) around the estuary (Huang, 1992). The BS is relatively shallow (an average 18m depth) and the largest inner sea of China with a total area of  $77,000 \text{ km}^2$ . Of the 17 rivers that discharge into the BS, the Yellow River is the most dominant because of its huge discharge of  $420 \times 10^8 \text{ m}^3 \text{ year}^{-1}$ , sediment load ( $10 \times 10^8 \text{ t year}^{-1}$ ), nutrients quantities in the following amounts –  $71.18 \text{ kt year}^{-1} \text{ NO}_3\text{-N}$  and  $0.43 \text{ kt year}^{-1} \text{ PO}_4\text{-P}$  (Zhang et al., 1994).

The *in situ* data collected from wide range of waters were used in the derivation of bio-optical algorithms for identifying ocean environmental parameters in the surface waters of the KSS, YS, and ECS. The *in situ* bio-optical measurements were performed during a lot of cruises conducted in the Korean seas and neighboring waters through the years 1998-2006 onboard the research vessels EARDO, Olympic, Tamgu, and Jangmok (Table 1). During each cruise, the water samples were collected with buckets/Niskin bottles and sub samples were filtered onboard onto Whatman GF/F glass microfiber filters for measurement of chlorophyll (chl), suspended sediments (SSC) and phytoplankton absorption ( $a_{ph}(\lambda)$ ). These filters were frozen at dark conditions until analysis took place at the laboratory with the standard spectrophotometric method for determining Chl and  $a_{ph}$  and oven-drying method for SSC (Kishino et al., 1984; Lee et al., 1998; Ahn et al., 2001). DOM absorption spectra were obtained from spectrophotometric method. Simultaneously, radiometric measurements such as downward spectral irradiance ( $E_d(\lambda)$ ) and total water leaving radiance ( $tL_w(\lambda)$ ) and sky radiance ( $L_{sky}(\lambda)$ ) were performed at various sample sites using an ASD FieldSpec Pro Dual VNIR Spectroradiometer with spectral range from 350-1050nm and spectral sample interval of 1.4nm. Most of these measurements were generally made in excellent conditions, near solar noon and under almost cloudless conditions. The data recorded in units of  $\text{mW cm}^{-2} \mu\text{m}^{-1} \text{ sr}^{-1}$  needed to be corrected for the contribution of sky-light reflection and air-sea interface effects (Ahn et al., 2001). Thus, the measured total water leaving radiance ( $tL_w(\lambda)$ ) was corrected for the sky light reflection and the air-sea interface.

### 3. Results and Discussion

The GOCI standard bio-optical algorithms are based on the simple regression between the field determinations of pigment concentration and spectral ratios of ocean re-

flectance or normalized water-leaving radiance.

#### 1) Chlorophyll

Several previous studies are the foundations for the development of new generation satellite ocean color sensors that are capable of detecting the sun-stimulated Chl-a fluorescence signal particularly in Case-2 waters, where suspended sediment particles (SS) and dissolved organic matter (DOM) can eventually interfere with estimation of Chl-a concentration using the standard band ratio algorithms (Clark, 1981; Babin *et al.*, 1996). The particular advantage of adopting fluorescence channels to estimate Chl-a concentration in aquatic system is that these channels are quite free from the influence of DOM, SS and strong atmospheric aerosol scattering, which are more pronounced at the shorter wavelength channels and therefore potential sources of errors in the standard blue/green ratio algorithms (Darecki and Stramski, 2004). Fluorescence algorithms are developed, using remote sensing reflectance spectra isolated for the wavelength range 660-730nm, on the basis of the following four variables: (1) the height of the fluorescence peak at 688 and 681nm ( $\Delta\text{Flu}$ ), (2) the area delimited by the  $\Delta\text{Flu}$  curve ( $\Delta\text{Flu}$ -Area) and (3) the fluorescence ratio ( $\Delta\text{Flu}$  (688/444)). These algorithms relies on the concept that Chl-a fluorescence increases the amount of water-leaving radiance signal at 688nm and 681 and decreases the signal at two wavelengths, 660nm and 730nm, on either side of this peak (Fig. 2).

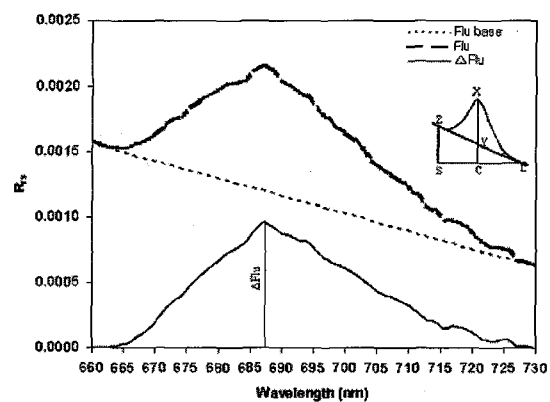
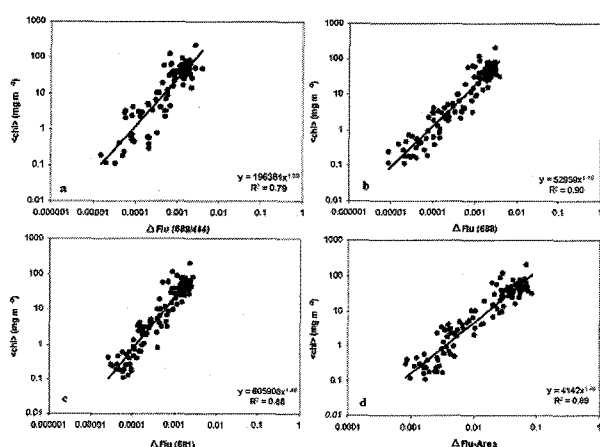


Fig. 2. Schematic representation of fluorescence line height (Flu) estimation from remote sensing fluorescence spectra. Thin and thick dotted lines represent the fluorescence base (Flu-base) and measured fluorescence (Flu) signal respectively, while thin solid line represents the estimated (Flu) fluorescence signal.

A statistical relationship was established between the  $\Delta\text{Flu}$  (688/444) ratio and *in situ* Chl-a concentrations (Fig. 3). Note that though a good correlation exists between these two parameters, data points show a wide scatter, especially at low and moderate Chl-a concentrations. The squared correlation coefficient ( $R^2$ ) of this relationship was observed to be lower (0.79) than that obtained from the relationship  $R_{rs}(444)/R_{rs}(554)$  and Chl-a concentrations. The wide scatter is thought to result

from variability in the yield of Chl-a fluorescence and perhaps the influence of DOM present in highly productive waters. Letelier and Abbott (1996) pointed out that several factors including phytoplankton species composition, nutrient availability, light intensity and temperature are responsible for variability in the yield of Chl-a fluorescence, leading to produce more errors to accurate estimation of Chl-a concentrations using the ratio  $\Delta\text{Flu}$  (688/444). On the contrary, the direct use of fluorescence signal is fairly straightforward and remains to be a practical one. Gower and his co-workers were among the first researchers to suggest the direct use of this signal to estimate Chl-a concentrations from aircraft and satellites. Figure 3 shows that the height of the peak at 688nm is highly correlated ( $R^2=0.90$ ) with the in-situ Chl-a concentrations. It is important to note that the use of the fluorescence line height at 688nm remains critical in satellite retrieval of Chl-a concentration because the  $O_2$  absorption feature is more pronounced at 687, leading to erode the long wavelength portion of the fluorescence peak. Alternatively, the second fluorescence maxima at 681 (adopted for MERIS and GLI) were regressed against in situ Chl-a concentrations. In log space, the squared correlation coefficient  $R^2$  is found to be slightly decreased from 0.90 ( $\Delta\text{Flu}(688)$ ) to 0.88 ( $\Delta\text{Flu}(681)$ ).



**Fig. 3.** *In-situ* Chl-a concentration ( $\text{mg m}^{-3}$ ) versus fluorescence-derived variables such as: (a) Flu (688/444), (b) Flu (688), (c) Flu (681), and (d) Flu-Area. The corresponding equation is as follows: (a)  $\langle \text{chl} \rangle$  ( $\text{mg m}^{-3}$ ) =  $196361 X^{1.30}$  with  $R^2 = 0.79$ , where  $X = \text{Flu}$  (688/444) (b)  $\langle \text{chl} \rangle$  ( $\text{mg m}^{-3}$ ) =  $52959 X^{1.15}$  with  $R^2 = 0.90$ , where  $X = \text{Flu}$  (688) (c)  $\langle \text{chl} \rangle$  ( $\text{mg m}^{-3}$ ) =  $605908 X^{1.48}$  with  $R^2 = 0.88$ , where  $X = \text{Flu}$  (681) (d)  $\langle \text{chl} \rangle$  ( $\text{mg m}^{-3}$ ) =  $4142 X^{1.46}$  with  $R^2 = 0.89$ , where  $X = \text{Flu-Area}$ . The total number of observations,  $N = 118$ .

The decrease in  $R^2$  value essentially results from the fact that at moderate and high Chl-a concentrations the height of the peak at this wavelength is often inevitably intermingled with each other, while there is a distinct signal for low Chl-a concentrations. To overcome this problem, it is recommended to use the area of fluorescence emission delimited above the baseline between 660 and 730nm because  $\Delta\text{Flu-Area}$  increases with increasing Chl-a concentration. A good correlation is ap-

parent through the regression analysis performed between these two variables, and the squared correlation coefficient increased monotonically from 0.88 to 0.89. The area based fluorescence algorithm remains valid, even when the physiological changes of phytoplankton result in changes in the magnitude of the fluorescence peak shifting towards longer part of the wavelength. This implies that the fluorescence-based algorithms are most effective in waters with various ranges of Chl-a concentrations, whereas the standard band ratio algorithms are more accurate in waters with very low ( $R_{rs}(443)/R_{rs}(555)$ ) and moderate ( $R_{rs}(490)/R_{rs}(555)$ ) Chl-a concentrations. Thus, the fluorescence algorithms might replace the requirement of the sophisticated band ratio algorithms for estimating Chl-a concentration, particularly in Case-2 waters, which are primarily dominated by the phytoplankton, suspended sediments of organic and inorganic origin and dissolved organic matter.

## 2) Suspended sediment

The surface sediment (SS) algorithm is derived from large data set containing remote sensing reflectance and *in situ* suspended sediment concentrations from a wide range of waters around Korean peninsula (Fig. 4). The suspended sediment concentration in surface waters normally range from  $0.2 \sim 120 \text{ g/m}^3$ . The present work did not attempt to derive band ratio algorithm because it has the poor performance in coastal waters where phytoplankton and other dissolved matters strongly influence this algorithm, particularly in the blue/green wavelength part of the spectrum. A reasonably strong relationship was observed between remote sensing reflectance at 555nm and an SS concentrations, which gives the empirical way of derivation of SS algorithm that can be expressed as follows,

$$\langle SS \rangle [\text{g/m}^3] = 441.6 [R_{rs}(555)]^{0.96} \quad (1)$$

with the squared correlation coefficient for log-transformed data,  $R^2 = 0.65$ , and the number of observations,  $n = 300$ . The SS concentration data set ranges between  $0.2\text{-}120 \text{ g/m}^3$ . This study did not attempt to derive algorithm based on blue-green wavelength ratios because it was found that band ratio algorithms are susceptible to failure in the presence of other optically active constituents such as particulate organic and dissolved matters (Ahn et al. 2001). The level of success of the red to green wavelength ratio is strongly influenced by the degree to which inorganic mineral sediments dominated the inherent optical properties of the water body. It is suggested, therefore, that the measurement of brightness through the use of single-band reflectance, rather than spectral ratios, may be the most reliable method for the derivation of suspended sediment concentrations in coastal/turbid waters.

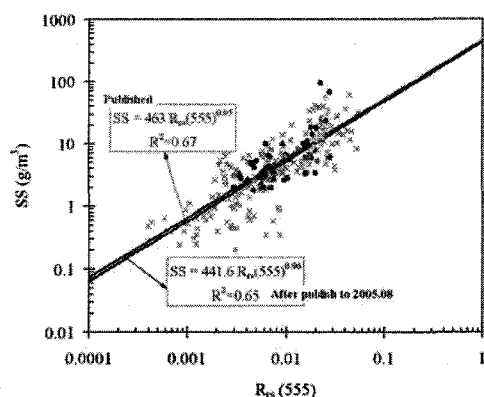


Fig. 4. Scatterplot of  $R_{rs}$  (555) versus SS concentration.

### 3) Colored dissolved organic matter

CDOM is a complex mixture of organic polymers derived from both terrestrial and marine sources, and consists of mostly soluble humic and fulvic substances that are yellow to brown in color. The effect of CDOM on the optical properties of the water is mainly to strongly absorb light in the UV and the blue end of the visible spectrum. Algorithms to measure CDOM using remote sensing images have been proposed in the past (Kahru and Mitchell, 2001; Chen et al., 2003). In this study, we are developing the DOM algorithm based on relationship  $a_{dom}(412)$  and ratio of  $R_{rs}(412)/R_{rs}(555)$ .

### Acknowledgement

This research was supported by Ministry of Maritime Affairs and Fisheries (MOMAF) under the KORDI contract PM 39700.

### References

[1] Morel, A., & Prieur, L. (1977). Analysis of variations in ocean color. *Limnology and Oceanography*, 22, 709-722.  
 [2] Gordon, H.R., & Morel, A. (1983). Remote assessment of ocean color for interpretation of satellite visible imagery-A review. In Barber, R.T., Bowman, M.J., Mooers, C.N.K., & Zetzel, B (Eds), Lecture notes on coastal and estuarine studies (pp. 1-144). New York: Springer-Verlag.  
 [3] Chang, K., Kim, Y.B., Suk, M.S., & Byun, S.K. (2002). Hydrography around Dokdo. *Ocean and Polar Research*, 24, 369-389.

[4] Lie, H.J., Cho, C.H., Lee, J.H., Niiler, P., & Hu, J.H. (1998). Separation of the Kuroshio water and its penetration onto the continental shelf west of Kyushu. *Journal of Geophysical Research*, 103, 2963-2976.  
 [5] Shen, Z., Lu, J., Liu, X., & Diao, H., 1992. Distribution characteristics of the nutrients in the Changjiang River estuary and the effect of the Three Gorges Project on it. *Studia Marina Sinica*, 39, 109-129.  
 [6] Gao, X., & Song, J. (2005). Phytoplankton distributions and their relationship with the environment in the Changjiang Estuary, China. *Marine Pollution Bulletin*, 50, 327-335.  
 [7] Huang, S. (1992). Management of Chinese estuaries. China Ocean Press, Beijing, pp. 156.  
 [8] Zhang, J., Hang, W., & Liu, M. (1994). Geochemistry of major Chinese river-estuary systems. In: Zhou, D., Liang, Y., & Tseng, C. (Eds.), *Oceanology of China Sea*. Kluwer Academic Publishers, The Netherlands, pp. 179-188.  
 [9] Kishino, M., Sugihara, S., & Okami, N. (1984). Estimation of quantum yield of chlorophyll a fluorescence from the upward irradiance spectrum in the sea. *La Mer.*, 22, 233-240.  
 [10] Ahn, y.h., Moon, J.E., & Gallegos, S. (2001). Development of suspended particulate matter algorithms for ocean color remote sensing. *Korean Journal of Remote Sensing*, 17, 285-295.  
 [11] Clark, D.K. 1981. Phytoplankton pigment algorithms for the Nimbus-7 CZCS. In J. F. R. Gower (ed.). *Oceanography from space*, Plenum. New York.  
 [12] Babin, m., Morel, A., and Gentili, B. 1996. Remote sensing of sea surface sun-induced chlorophyll-a fluorescence: Consequences of natural variation in the optical characteristics of phytoplankton and the quantum yield of chlorophyll a fluorescence. *International Journal of Remote Sensing*, 17, 2417-2448.  
 [13] Darecki, M., & Stramski, D. (2004). An evaluation of MODIS and SeaWiFS bio-optical algorithms in the Baltic Sea. *Remote Sensing of Environment*, 89, 326-350.  
 [14] Letelier, R. M., and Abbott, M. R. 1996. An analysis of chlorophyll-a fluorescence algorithms for the moderate resolution imaging spectrometer (MODIS). *Remote Sensing of Environment*, 58, 215-223.  
 [15] O'Reilly, J.E., Moritorena, S., Mitchell, B.G., Seigel, D.A., Carder, K.L., Garver, S.A., Kahru, M., & McClain, C. (1998). Ocean color chlorophyll algorithms for SeaWiFS. *Journal of Geophysical Research*, 103, 24,937-24953.